

Synthesis and Characterization of the Dinuclear Polyhydrides $[\text{Os}_2\text{H}_7(\text{PPh}'\text{Pr}_2)_4]^+$ and $[\text{Os}_2\text{H}_6(\text{PPh}'\text{Pr}_2)_4]$

Bradley G. Anderson,* Sarah A. Hoyte, and John L. Spencer*

School of Chemical and Physical Sciences, Victoria University of Wellington, Wellington, New Zealand

Received January 19, 2009

The dinuclear osmium polyhydride $[\text{Os}_2\text{H}_7(\text{PPh}'\text{Pr}_2)_4][\text{HC}(\text{SO}_2\text{CF}_3)_2]$ (**1**) was synthesized by the protonation of $[\text{OsH}_6(\text{PPh}'\text{Pr}_2)_2]$ with bis(trifluoromethylsulfonyl)methane. Treatment with amine bases was not able to deprotonate **1**, but reaction with potassium hydride gave the corresponding neutral polyhydride $[\text{Os}_2\text{H}_6(\text{PPh}'\text{Pr}_2)_4]$ (**2**). Single crystal X-ray diffraction revealed that **1** and **2** both crystallize in the $P2_1/c$ space group and are classical polyhydrides containing similar $\text{Os}(\mu\text{-H})_2\text{Os}$ cores with Os–Os distances of 2.5431(1) Å and 2.5448(2) Å, respectively. These structures represent rare examples of dinuclear osmium polyhydrides with six or more hydride ligands.

Introduction

Dinuclear transition metal polyhydride complexes have been known since complexes of the type $\text{Re}_2\text{H}_8\text{P}_4$ (where P is a phosphorus-donor ligand such as a phosphine) were first reported by Chatt and Coffey in 1969.¹ Since then homo- and heterodinuclear polyhydrides of a range of metals including molybdenum, ruthenium, and platinum have been synthesized.² Of these species, many of the most interesting complexes have a relatively large hydride count of between six and nine hydride ligands. A high hydride count means these complexes require a low number of ancillary ligands for stabilization, giving them a versatile chemistry based around loss of molecular hydrogen and reaction with donor molecules.²

Much of the research in this field has focused on dinuclear polyhydrides of rhenium and ruthenium,^{3–6} with comparatively little work reported on similar diosmium polyhydrides. Consequently there are few reports of diosmium compounds with high hydride counts, such as the pentahydride $[\text{Cp}^*\text{Os}_2\text{H}_5]^+$.⁷

Herein we report the synthesis and characterization of the dinuclear osmium heptahydride, $[\text{Os}_2\text{H}_7(\text{PPh}'\text{Pr}_2)_4]^+$ (**1**), synthesized via the protonation of a mononuclear precursor rather than the photochemical methods conventionally used to produce diosmium polyhydrides. We also report the deprotonation of **1** to form the first diosmium hexahydride,

$[\text{Os}_2\text{H}_6(\text{PPh}'\text{Pr}_2)_4]$ (**2**) (Scheme 1), as well as the X-ray crystal structures of both species.

Experimental Section

All reactions were carried out using degassed solvents and standard Schlenk techniques under a nitrogen atmosphere. Starting materials were purchased from Sigma-Aldrich and used without further purification unless otherwise stated. Bis(trifluoromethylsulfonyl)methane⁸ and $[\text{OsH}_6(\text{PPh}'\text{Pr}_2)_2]$ ⁹ were synthesized via previously reported methods. NMR solvents were purchased from Sigma-Aldrich and stored under nitrogen. NMR spectra were measured on Varian Unity Inova 300 and 500 MHz NMR spectrometers, with chemical shift values δ referenced to the residual solvent peaks for ¹H and to 85% H_3PO_4 for ³¹P. All IR spectra were obtained on a Perkin-Elmer Spectrum One FT-IR Spectrometer using KBr disks. Elemental analyses were performed by the Campbell Microanalytical Laboratory, University of Otago, New Zealand.

Protonation of $[\text{OsH}_6(\text{PPh}'\text{Pr}_2)_2]$ - Synthesis of $[\text{Os}_2\text{H}_7(\text{PPh}'\text{Pr}_2)_4][\text{HC}(\text{SO}_2\text{CF}_3)_2]$ (1**).** $\text{H}_2\text{C}(\text{SO}_2\text{CF}_3)_2$ (49 mg, 0.17 mmol) was reacted with $[\text{OsH}_6(\text{PPh}'\text{Pr}_2)_2]$ (101 mg, 0.17 mmol) in dichloromethane (5 mL) for 20 h. The solvent was removed in vacuo, leaving a dark yellow oil. Addition of diethyl ether (15 mL) yielded the product as air stable dark red microcrystals (0.11 g, 86%). ¹H NMR (CD_2Cl_2): δ 7.22 ppm (m, 20H, PC_6H_5), 3.90 (s, 1H, $\text{HC}(\text{SO}_2\text{CF}_3)_2$), 2.00 (br s, 8H, PCH), 1.00 (br s, 48H, CH_3), –8.93 (q, $J_{\text{P-H}} = 8.4$ Hz, 3H, bridging OsH), –12.92 (t, $J_{\text{P-H}} = 28$ Hz, 4H, terminal OsH). ³¹P NMR (CD_2Cl_2): δ 50.1 ppm (s). IR (KBr, cm^{-1}): $\nu(\text{OsH})$ 2140 (w, br). Elemental Analysis: $\text{C}_{51}\text{H}_{84}\text{O}_4\text{F}_6\text{P}_4\text{S}_2\text{Os}_2$ requires C, 42.4; H, 5.9%. Found: C, 42.5; H, 6.0%.

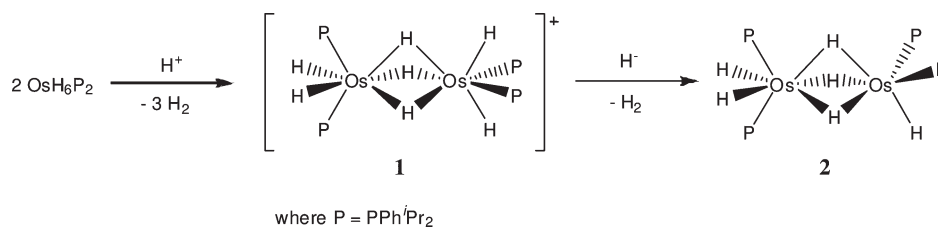
Deprotonation of $[\text{Os}_2\text{H}_7(\text{PPh}'\text{Pr}_2)_4]^+$ - Synthesis of $[\text{Os}_2\text{H}_6(\text{PPh}'\text{Pr}_2)_4]$ (2**).** $[\text{Os}_2\text{H}_7(\text{PPh}'\text{Pr}_2)_4][\text{HC}(\text{SO}_2\text{CF}_3)_2]$ (300 mg, 0.21 mmol) was added to a suspension of potassium hydride (27 mg, 0.67 mmol) in sodium-dried THF (20 mL). The mixture was

*To whom correspondence should be addressed. E-mail: andersbrad@myvuw.ac.nz (B.G.A.), john.spencer@vuw.ac.nz (J.L.S.).

(1) Chatt, J.; Coffey, R. S. *J. Chem. Soc. A* **1969**, 1963–1972.
(2) Hlatky, G. G.; Crabtree, R. H. *Coord. Chem. Rev.* **1985**, *65*, 1–48.
(3) Allison, J. D.; Walton, R. A. *J. Am. Chem. Soc.* **1984**, *106*, 163–168.
(4) Ito, J.; Shima, T.; Suzuki, H. *Organometallics* **2004**, *23*, 2447–2460.
(5) Suzuki, H. *Eur. J. Inorg. Chem.* **2002**, 2002, 1009–1023.
(6) Chaudret, B.; Devillers, J.; Poilblanc, R. *Organometallics* **1985**, *4*, 1727–1732.
(7) Kameo, H.; Suzuki, H. *Organometallics* **2008**, *27*, 4248–4253.

(8) Koshar, R. J.; Mitsch, R. A. *J. Org. Chem.* **1973**, *38*, 3358–3363.
(9) Connelly, N. G.; Howard, J. A. K.; Spencer, J. L.; Woodley, P. K. *J. Chem. Soc., Dalton Trans.* **1984**, 2003–2009.

Scheme 1



stirred for 1 hour, after which the supernatant liquid was removed and dried in vacuo to yield a dark brown expanded oil. Recrystallization from diethyl ether yielded dark red microcrystals that decomposed when exposed to the atmosphere. ¹H NMR (C₆D₆): δ 7.51 ppm (m, 8H, PC₆H₅), 6.91 (m, 12H, PC₆H₅), 2.07 (sext, *J*_{H-H} = 6.9 Hz, 8H, PCH), 1.29 (dd, *J*_{P-H} = 15.0 Hz, *J*_{H-H} = 6.9 Hz, 24H, CH₃), 1.05 (dd, *J*_{P-H} = 15.0 Hz, *J*_{H-H} = 6.9 Hz, 24H, CH₃), -12.63 (s, 6H, OsH). ³¹P NMR (C₆D₆): δ 48.2 ppm (s).

Observation of the Protonation Intermediate [OsH₇(PPhⁱPr₂)₂]⁺ (3). Dichloromethane-*d*₂ was added to a mixture of [OsH₆(PPhⁱPr₂)₂] (20 mg, 0.034 mmol) and H₂C(SO₂CF₃)₂ (10 mg, 0.036 mmol) in a stoppered NMR tube under nitrogen at 195 K. Quantitative formation of **1** was complete after about 30 min, at which point the yellow solution was analyzed by NMR. Above approximately 253 K **3** reacts irreversibly to form a dark red solution of **1**. ¹H NMR (CD₂Cl₂, 243 K): δ 7.64 ppm (m, 4H, PC₆H₅), 7.54 (m, 6H, PC₆H₅), 3.85 (br s, 1H, HC(SO₂CF₃)₂), 2.44 (m, 4H, PCH), 1.03 (m, 12H, CH₃), 0.99 (m, 12H, CH₃), -6.49 (s, 7H, OsH). ³¹P NMR (CD₂Cl₂, 243 K): δ 33.8 ppm (s).

X-ray Structure Analysis. Red block crystals of **1** were obtained after two days from the slow diffusion of diethyl ether into a dichloromethane solution of **1**. Dark red block crystals of **2** were obtained by recrystallization from diethyl ether. X-ray diffraction data was collected on a Bruker SMART CCD diffractometer using Mo K α radiation. Data was reduced using Bruker SAINT software. Absorption correction was performed using the SADABS program. The structures were solved by direct methods using SHELXS97 and refined using SHELXL97.¹⁰ All atoms were located during refinement.

Results

Protonation of [OsH₆(PPhⁱPr₂)₂] - Synthesis and Characterization of [Os₂H₇(PPhⁱPr₂)₄][HC(SO₂CF₃)₂]. The reaction of [OsH₆(PPhⁱPr₂)₂] with 1 equiv of H₂C(SO₂CF₃)₂ in CH₂Cl₂ yielded dark red microcrystals of **1** upon removal of the solvent and treatment with diethyl ether. NMR analysis of **1** showed a signal in the ³¹P NMR spectrum at 50.1 ppm and two hydride resonances at -9.82 (quintet) and -12.93 ppm (triplet) in the ¹H NMR spectrum.

The coupling patterns of these hydride resonances suggested a hydride-bridged dinuclear species. The observation of hydride environments coupled to two and four phosphorus atoms (a triplet and a quintet) indicated the presence of bridging and terminal hydrides. Integration of the hydride resonances against those of the phosphine ligands in the ¹H NMR spectrum indicated that four phosphine ligands, three bridging hydrides and four terminal hydrides were present. Upon lowering the temperature to 193 K the two hydride resonances broadened, but did not decoalesce. The conjugate base of

bis(trifluoromethylsulfonyl)methane was observed in the ¹H NMR spectrum at 3.90 ppm in a 1:1 ratio with **1**. This chemical shift was consistent with previous observations of non-coordinated HC(SO₂CF₃)₂⁻,¹¹ and confirmed the cationic nature of the product.

Performing the protonation reaction in situ in an NMR tube showed that initially an intermediate species (**3**) was formed, which displayed a ³¹P NMR resonance at 33.8 ppm and a broad singlet ¹H NMR resonance at -6.49 ppm. After 3 h at room temperature, this species had been completely replaced by **1**. Further investigation revealed that **3** was indefinitely stable in CD₂Cl₂ solution below 253 K. Repeating this reaction at 193 K allowed formation of **3** without further reaction to form **1**. Integration of the signals indicated that **3** had seven hydride and two phosphine ligands, suggesting the chemical formula [OsH₇(PPhⁱPr₂)₂]⁺.

Measurement of the spin-lattice relaxation time *T*₁ performed on **3** gave a value of 22.0 ms¹² at 193 K (the lower temperature limit of the probe). Obtaining *T*₁ values at 193 K (22.0 ms), 203 K (27.6 ms), 213 K (35.0 ms), and 243 K (69.7 ms) allowed us to estimate that *T*_{1 min} would be in the vicinity of 17 ms at 170 K. This is significantly shorter than *T*_{1 min} for the starting material (116 ms).¹³ Care needs to be exercised when assigning non-classical structures on the basis of *T*₁ measurements. It has been demonstrated that metal-hydride and ligand-hydride interactions can contribute significantly to the observed hydride relaxation rate (*R*_{obs}, 1/*T*₁), leading to a low *T*_{1 min} value without the presence of a molecular hydrogen ligand.¹³ This has led to classical polyhydrides being mistakenly characterized as molecular hydrogen species^{14,15} on the basis of short *T*_{1 min} values (<100 ms).¹⁶ For **3** the metal-hydride and ligand-hydride interactions can be approximated by using the values from [OsH₆(PPhⁱPr₂)₂] (adjusted to 300 MHz)¹³ and are responsible for less than 7% of the value of *R*_{obs}, meaning that the observed *T*₁ should be predominantly due to H-H dipole interactions among the hydride ligands. With a *T*₁ of 22.0 ms (193 K) and a predicted *T*_{1 min} of 17 ms, significantly lower than the < 35 ms value associated with non-classical polyhydrides,¹⁵ we are confident that [OsH₇(PPhⁱPr₂)₂]⁺ possesses a non-classical structure.

(11) Siedle, A. R.; Newmark, R. A.; Pignolet, L. H. *Inorg. Chem.* **1986**, *25*, 3412–3418.

(12) All *T*₁ measurements performed at 300 MHz, with literature values adjusted to 300 MHz for comparison.

(13) Desrosiers, P. J.; Cai, L.; Lin, Z.; Richards, R.; Halpern, J. *J. Am. Chem. Soc.* **1991**, *113*, 4173–4184.

(14) Cotton, F. A.; Luck, R. L. *J. Am. Chem. Soc.* **1989**, *111*, 5757–5761.

(15) Luo, X. L.; Crabtree, R. H. *Inorg. Chem.* **1989**, *28*, 3775–3777.

(16) Hamilton, D. G.; Crabtree, R. H. *J. Am. Chem. Soc.* **1988**, *110*, 4126–4133.

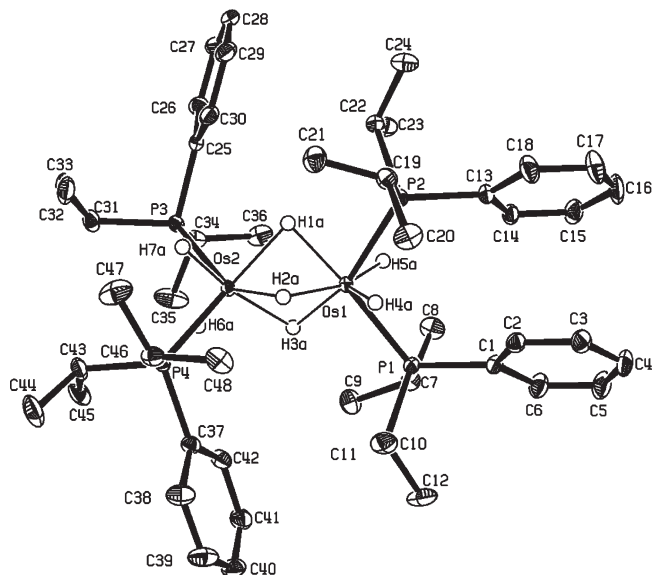


Figure 1. ORTEP diagram of **1** showing 50% probability thermal ellipsoids. Non-hydride H-atoms and the $\text{HC}(\text{SO}_2\text{CF}_3)_2^-$ anion have been omitted for clarity.

The NMR data obtained for **3** is similar to that reported for an analogous cationic heptahydride, $[\text{OsH}_3(\text{H}_2)_2(\text{P}^i\text{Pr}_3)_2]^+$.¹⁷ This compound displayed a T_1 min of 12.2 ms (169 K), compared to a value of 119 ms for the parent $[\text{OsH}_6(\text{P}^i\text{Pr}_3)_2]$ species. The bis(dihydrogen) structure was elucidated on the basis of T_1 min data and J_{HD} coupling values in the η^2 -HD ligand of the d_6 isotopomer. Given the similarities between the two compounds, the structure of **3** is thought to be the bis(dihydrogen) polyhydride $[\text{OsH}_3(\text{H}_2)_2(\text{PPh}^i\text{Pr}_2)_2]^+$.

X-ray Crystal Structure of $[\text{Os}_2\text{H}_7(\text{PPh}^i\text{Pr}_2)_4][\text{HC}(\text{SO}_2\text{CF}_3)_2]$. Crystals of a quality sufficient for use in X-ray analysis were grown by the inward diffusion of diethyl ether into a dichloromethane solution of the crude reaction product. Single crystal X-ray crystallography confirmed the proposed structure of **1**, showing a dinuclear species composed of two OsP_2H_2 fragments bridged by a $(\mu\text{-H})_3$ face (Figure 1). The Os–Os distance of 2.5431(1) Å (Table 1) is consistent with the $\text{Os}_2(\mu\text{-H})_3$ structure, being similar to the Os–Os distances in the hydride-bridged species $[\text{Os}_2\text{H}_4(\text{PMePh}_2)_5]$ and $[\text{Os}_2\text{H}_3(\text{PMe}_2\text{Ph})_6]^+$ (2.551(1) and 2.558(1) Å, respectively).^{18,19} The two OsP_2H_2 units are staggered about the Os–Os bond, having an average torsion angle of 61.77°. The average P–Os–P angle is 112.6°, and the average Os–P bond length is 2.32 Å (Table 1). In the starting material $[\text{OsH}_6(\text{PPh}^i\text{Pr}_2)_2]$ the P–Os–P angle is 155.2(1)° and Os–P distance is 2.342(7) Å.²⁰

The $\text{HC}(\text{SO}_2\text{CF}_3)_2^-$ counterion is non-coordinating. The nearest contact of 2.50 Å between O(4) of the SO_2CF_3 group and an aromatic H on C(40) is similar to that observed in $[\text{OsH}_3(\text{PPh}_3)_4][\text{HC}(\text{SO}_2\text{CF}_3)_2]$ (2.47 Å)¹¹ and

Table 1. Crystallographic Data for $[\text{Os}_2\text{H}_7(\text{PPh}^i\text{Pr}_2)_4][\text{HC}(\text{SO}_2\text{CF}_3)_2]$ (**1**):

chemical formula	$\text{C}_{51}\text{H}_{84}\text{O}_4\text{F}_6\text{P}_4\text{S}_2\text{Os}_2$
formula weight	1443.58
<i>a</i> , Å	17.1709(5)
<i>b</i> , Å	22.0917(6)
<i>c</i> , Å	16.7632(4)
α , deg	90
β , deg	112.3520(10)
γ , deg	90
<i>V</i> , Å ³	5881.1(3)
<i>Z</i>	4
space group	$P2_1/c$
<i>T</i> , K	97
λ	0.71073
d_{calcd} , g cm ⁻³	1.63
μ , cm ⁻¹	4.556
R_1 ($I > 2\sigma(I)$) ^a	0.0200
wR_2 (all data) ^a	0.0466

Selected Bond Distances (Å) and Angles (deg) for Complex **1**

Os(1)–Os(2)	2.54306(12)	Os(1)–P(1)	2.3209(5)
Os(1)–P(2)	2.3179(5)	Os(2)–P(3)	2.3233(5)
Os(2)–P(4)	2.3250(5)	Os(1)–H(1A)	1.837
Os(2)–H(1A)	1.906	Os(1)–H(2A)	1.744
Os(2)–H(2A)	1.770	Os(1)–H(3A)	1.734
Os(2)–H(3A)	1.786	Os(1)–H(4A)	1.398
Os(1)–H(5A)	1.512	Os(2)–H(6A)	1.519
Os(2)–H(7A)	1.564		
Os(2)–Os(1)–P(1)	124.758(13)	Os(2)–Os(1)–P(2)	122.851(12)
Os(1)–Os(2)–P(3)	122.520(12)	Os(1)–Os(2)–P(4)	124.364(12)
P(1)–Os(1)–P(2)	112.276(17)	P(3)–Os(2)–P(4)	112.998(17)
Os(2)–Os(1)–H(4A)	118.73	Os(2)–Os(1)–H(5A)	119.90
Os(1)–Os(2)–H(6A)	121.36	Os(1)–Os(2)–H(7A)	121.77
P(1)–Os(1)–H(4A)	74.81	P(1)–Os(1)–H(5A)	74.93
P(2)–Os(1)–H(4A)	70.91	P(2)–Os(1)–H(5A)	76.02
P(3)–Os(2)–H(6A)	70.81	P(3)–Os(2)–H(7A)	73.24
P(4)–Os(2)–H(6A)	72.68	P(4)–Os(2)–H(7A)	76.09
H(4A)–Os(1)–H(5A)	121.31	H(6A)–Os(2)–H(7A)	116.74
Os(1)–H(1A)–Os(2)	85.57	Os(1)–H(2A)–Os(2)	92.72
Os(1)–H(3A)–Os(2)	92.51		

^a Definition of R indices: $R_1 = \sum ||F_o| - |F_c|| / \sum |F_o|$; $wR_2 = [\sum w(F_o^2 - F_c^2)^2 / \sum w(F_o^2)^2]^{1/2}$.

is presumably due to the constraints of the crystal packing rather than any association.

Deprotonation of $[\text{Os}_2\text{H}_7(\text{PPh}^i\text{Pr}_2)_4][\text{HC}(\text{SO}_2\text{CF}_3)_2]$ - Synthesis and Characterization of $[\text{Os}_2\text{H}_6(\text{PPh}^i\text{Pr}_2)_4]$. Crystals of **1** were added to a suspension of potassium hydride in tetrahydrofuran (THF), producing a solution that formed a dark brown expanded oil when the solvent was removed under vacuum. Recrystallization from diethyl ether yielded dark red microcrystals of **2**. The ³¹P NMR spectrum of **2** showed a single peak at 48.2 ppm and a singlet hydride resonance at -12.63 ppm in the ¹H NMR spectrum at room temperature. Integration data indicated that **2** contained four phosphine ligands and six hydrides.

To confirm that six hydride ligands were present, elucidation of the P–H coupling patterns was attempted by performing selective proton-decoupled ³¹P NMR spectroscopy. However, the ³¹P resonance remained a singlet both at room temperature and at 348 K. In contrast, resolution of the P–H coupling was achieved using variable temperature ¹H NMR. Upon increasing the temperature to 333 K, the hydride peak showed coupling to four phosphorus nuclei (quintet, $J_{\text{P-H}} = 2.5$ Hz) (Figure 2), demonstrating that **2** is a dinuclear polyhydride with rapidly exchanging bridging and terminal hydrides. Low temperature ¹H NMR spectroscopy

(17) Smith, K.-T.; Tilset, M.; Kuhlman, R.; Caulton, K. G. *J. Am. Chem. Soc.* **1995**, *117*, 9473–9480.

(18) Bruno, J. W.; Huffman, J. C.; Green, M. A.; Zubkowski, J. D.; Hatfield, W. E.; Caulton, K. G. *Organometallics* **1990**, *9*, 2556–2567.

(19) Green, M. A.; Huffman, J. C.; Caulton, K. G. *J. Organomet. Chem.* **1983**, *243*, C78–C82.

(20) Howard, J. A. K.; Johnson, O.; Koetzle, T. F.; Spencer, J. L. *Inorg. Chem.* **1987**, *26*, 2930–2933.

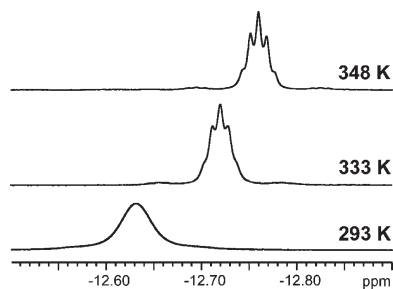


Figure 2. Variable temperature ^1H NMR spectra of **2**.

confirmed the presence of six hydride ligands, with the observation of three broad singlet resonances at -10.45 , -12.95 , and -21.02 ppm in a 3:2:1 ratio at 193 K (Figure 3). This allows a formulation of **2** as an unsymmetrical dinuclear polyhydride with three bridging and three terminal hydrides.

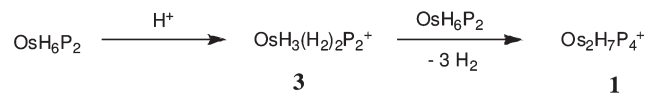
X-ray Crystal Structure of $[\text{Os}_2\text{H}_6(\text{PPh}^i\text{Pr}_2)_4]$. Recrystallization of **2** from diethyl ether yielded dark red rectangular prisms of sufficient quality for single crystal X-ray diffraction analysis. The dimer is unsymmetrical, composed of OsP_2H and OsP_2H_2 fragments sharing a common $(\mu\text{-H})_3$ face (Figure 4). The six-coordinate osmium Os(1) is a distorted octahedron, with a $\text{P}(1)\text{-Os}(1)\text{-P}(2)$ angle of $105.29(3)^\circ$, while the additional terminal hydride at the seven-coordinate osmium forces a $\text{P}(3)\text{-Os}(2)\text{-P}(4)$ angle of $113.76(3)^\circ$ (Table 2). The Os–Os distance is consistent with other trihydride-bridged diosmium structures at $2.5447(2)$ Å,¹⁸ and is very similar to the Os–Os bond length in **1** (only 0.06% difference between the two).

Discussion

Synthesis of $[\text{Os}_2\text{H}_7(\text{PPh}^i\text{Pr}_2)_4]^+$ (1**).** The protonation of $[\text{OsH}_6(\text{PPh}^i\text{Pr}_2)_2]$ to form **1** represents the first example of dinuclear osmium polyhydride formation through the protonation of a mononuclear precursor. This protonation is analogous to the chemistry of rhenium polyhydrides, where polyhydrides of the type ReH_7P_2 can be protonated to form $\text{Re}_2\text{H}_9\text{P}_4^+$.^{21,22} It is also similar to the protonation of the osmium halohydride $\text{OsH}_2\text{Cl}_2\text{P}_2$, which forms the chloride-bridged $\text{P}_2\text{H}_2\text{Os}(\mu\text{-Cl})_3\text{OsH}_2\text{P}_2^+$ through elimination of HCl .²³

Previously, dinuclear osmium polyhydrides such as $\text{Os}_2\text{-H}_4\text{P}_6$, $\text{Os}_2\text{H}_4\text{P}_5$, and $[\text{Cp}^*\text{Os}_2\text{H}_4]$ have been generated by photolysis rather than protonation,^{18,24} with cationic dinuclear osmium polyhydrides obtained through the protonation of these photolysis products.^{7,19} Where the protonation of mononuclear osmium polyhydrides has been attempted, the products are reported to be mononuclear polyhydrides.^{11,17} In a reaction analogous to that of the formation of **1**, $[\text{OsH}_6(\text{P}^i\text{Pr}_3)_2]$ was protonated with HBF_4 to yield the non-classical polyhydride $[\text{OsH}_3(\text{H}_2)_2(\text{P}^i\text{Pr}_3)_2]^+$.¹⁷

Scheme 2



Very recently a brief report²⁵ has appeared describing the thermal decomposition of $[\text{OsH}_3(\text{H}_2)_2(\text{P}^i\text{Pr}_3)_2]^+$ at reflux in toluene, leading to the formation of $[\text{Os}_2\text{H}_7(\text{P}^i\text{Pr}_3)_4]^+$ which is similar to **1**.

This difference in reactivity is most likely due to the different electronic effects of the diisopropylphenyl and the triisopropyl phosphine ligands, with PPh^iPr_2 being a poorer σ -donor than P^iPr_3 (σ -donor capacity, $\chi_{\text{d}} = 10$ for PPh^iPr_2 , 3.45 for P^iPr_3).²⁶ This means the PPh^iPr_2 ligand produces an $[\text{OsH}_3(\text{H}_2)_2\text{P}_2]^+$ intermediate (**3**) with a less electron rich osmium atom, reducing the amount of Os-H_2 backbonding and making H_2 more labile. This trend of complexes with stronger σ -donor ligands exhibiting reduced H_2 dissociation has previously been observed for $[\text{OsH}_5(\text{PPh}_3)_3]^+$ and $[\text{OsH}_5(\text{PPhMe}_2)_3]^+$ species, with the more weakly donating PPh_3 ligand promoting H_2 elimination 2 orders of magnitude faster than the more strongly donating PPhMe_2 .²⁷ Thus, the increased propensity for H_2 dissociation with the less donating PPh^iPr_2 ligand facilitates the formation of **1** in a reaction that involves the loss of three molecules of hydrogen (Scheme 2).

Compounds **1** and **2** could be assigned Os–Os triple-bonds within the $\text{Os}_2(\mu\text{-H})_3$ cores on the basis of the EAN rule, Os–Os distances in the solid state structures and consistency with similar work.^{4,18,19,28} However it must be noted that for similar 30-electron species $[\text{Cp}^*\text{Ru}_2(\mu\text{-H})_4]$ and $[(\eta^6\text{-C}_6\text{Me}_6)_2\text{Ru}_2(\mu\text{-H})_3]^+$, quantum mechanical computations have demonstrated that there is minimal direct orbital interaction between the metal centers, with the metal–metal distances in the solid state structures being a result of the geometric constraints imposed by the bridging hydrides.^{29,30} Assigning these type of structures a metal–metal triple bond can be useful in rationalizing bond lengths and observed reactivities;³⁰ however, comparisons between these structures and those with unbridged Os–Os triple bonds should be made with caution.

The structure of **1** (and the recently prepared²⁵ $[\text{Os}_2\text{H}_7(\text{P}^i\text{Pr}_3)_4]^+$) is interesting in two respects. It has the highest reported oxidation state for osmium in a $\text{Os}_2(\mu\text{-H})_3$ configuration (Os^{4+}).³¹ The other examples of bimetallic $\text{Os}_2(\mu\text{-H})_3$ osmium species all contain Os^{2+} ,^{18,19,32,33} while an Os_5 cluster contains a $(\mu\text{-H})_3$ face bridging Os^{2+} and Os^{3+} atoms.³⁴ High oxidation state $\text{M}_2(\mu\text{-H})_3$ bridges are uncommon for ruthenium species as well, the highest

(26) Fernandez, A. L.; Wilson, M. R.; Prock, A.; Giering, W. P. *Organometallics* **2001**, *20*, 3429–3435.

(27) Jessop, P. G.; Morris, R. H. *Coord. Chem. Rev.* **1992**, *121*, 155–284.

(28) Tschan, M. J.-L.; Chérioux, F.; Therrien, B.; Süß-Fink, G. *Eur. J. Inorg. Chem.* **2007**, *2007*, 509–513.

(29) Koga, N.; Morokuma, K. *J. Mol. Struct.* **1993**, *300*, 181–189.

(30) Fowe, E. P.; Therrien, B.; Süß-Fink, G.; Daul, C. *Inorg. Chem.* **2008**, *47*, 42–48.

(31) Results of a Cambridge Structural Database search for the $\text{Os}_2(\mu\text{-H})_3$ structural unit.

(32) Schulz, M.; Stahl, S.; Werner, H. *J. Organomet. Chem.* **1990**, *394*, 469–479.

(33) Therrien, B.; Vieille-Petit, L.; Süß-Fink, G. *J. Mol. Struct.* **2005**, *738*, 161–163.

(34) Li, Y.; Wong, W.-T. *Dalton Trans.* **2003**, 398–405.

(21) Bravo, J.; Castro, J.; García-Fontán, S.; Iglesias, M.; Rodríguez-Seoane, P. *J. Organomet. Chem.* **2005**, *690*, 4899–4907.

(22) Love, J. B. Heterobimetallic Polyhydride and Alkyl Polyhydride Complexes of Rhenium. PhD Thesis, University of Salford, Salford, U.K., **1993**.

(23) Kuhlman, R.; Streib, W. E.; Caulton, K. G. *Inorg. Chem.* **1995**, *34*, 1788–1792.

(24) Gross, C. L.; Girolami, G. S. *Organometallics* **2007**, *26*, 160–166.

(25) Buil, M. L.; Esteruelas, M. A.; Garcés, K.; García-Raboso, J.; Oliván, M. *Organometallics* **2009**, ASAP DOI: 10.1021/om9002544.

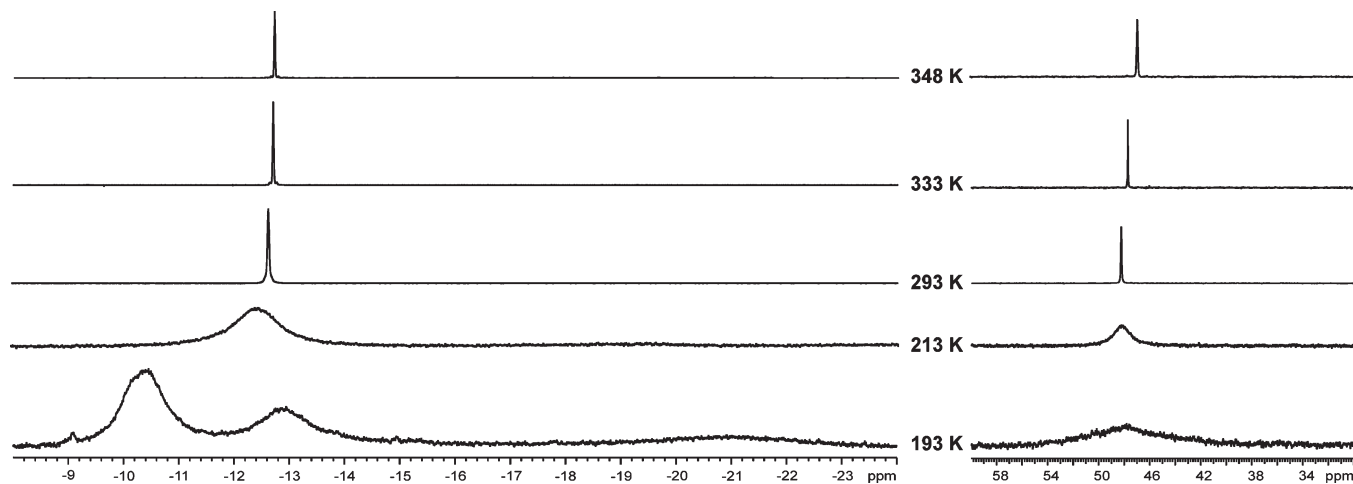


Figure 3. Variable temperature ^1H (left) and ^{31}P (right) NMR spectra of **2**.

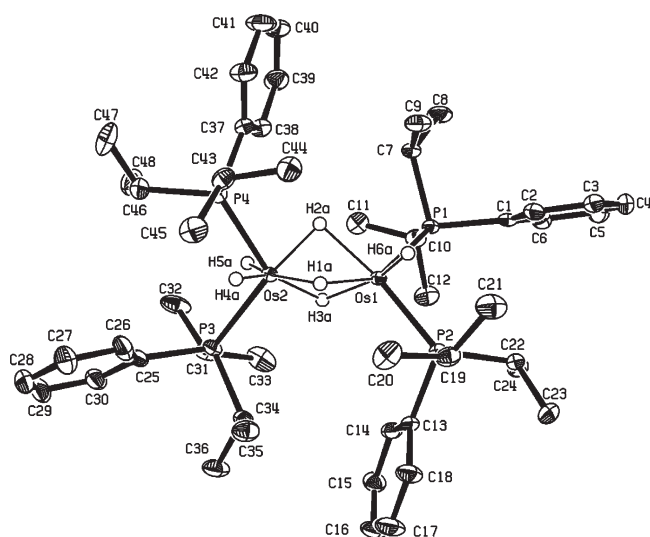


Figure 4. ORTEP diagram of **2** showing 50% probability thermal ellipsoids. Non-hydride H-atoms omitted for clarity.

being Ru^{3+} in $[\text{Ru}_2\text{H}_6(\text{P}^i\text{Pr}_3)_4]^{35,36}$. Second, **1** (along with $[\text{OsH}_7(\text{P}^i\text{Pr}_3)_4]^+$) has the highest hydride content of all reported dinuclear species (7 hydride ligands), surpassing the previous mark of 5 hydride ligands in $[\text{Cp}^*\text{Os}_2\text{H}_5][\text{BF}_4]$.³ Compound **1**, however, has fewer hydrides per osmium than Bronger's monooxmium $[\text{OsH}_7]^{3-}$ and $[\text{OsH}_9]^{3-}$ species.³⁷

Synthesis of $[\text{Os}_2\text{H}_6(\text{PPh}^i\text{Pr}_2)_4]$ (2**).** Deprotonation of the dinuclear polyhydride **1** was viewed as a route to the synthesis of the neutral hexahydride **2**, as reversible protonation has been observed for dinuclear rhenium octahydrides of the type $\text{Re}_2\text{H}_8\text{P}_4$.³⁸ The corresponding dinuclear ruthenium hexahydrides $\text{Ru}_2\text{H}_6\text{P}_4$ have been known in the literature since 1985,⁶ and can be

Table 2. Crystallographic Data for $[\text{Os}_2\text{H}_6(\text{PPh}^i\text{Pr}_2)_4]$ (**2**):

chemical formula	$\text{C}_{48}\text{H}_{82}\text{P}_4\text{Os}_2$
formula weight	1163.42
a , Å	17.9836(6)
b , Å	15.1146(5)
c , Å	18.9267(6)
α , deg	90
β , deg	106.994(2)
γ , deg	90
V , Å ³	4919.9(3)
Z	4
space group	$P2_1/c$
T , K	119
λ	0.71073
d_{calcd} , g cm ⁻³	1.57
μ , cm ⁻¹	5.321
R_1 ($I > 2\sigma(I)$) ^a	0.0318
wR_2 (all data) ^a	0.0715

Selected Bond Distances (Å) and Angles (deg) for Complex **2**

Os(1)–Os(2)	2.54471(18)	Os(1)–P(1)	2.2645(7)
Os(1)–P(2)	2.2736(8)	Os(2)–P(3)	2.3113(8)
Os(2)–P(4)	2.3169(8)	Os(1)–H(1A)	1.712
Os(2)–H(1A)	1.735	Os(1)–H(2A)	1.872
Os(2)–H(2A)	1.663	Os(1)–H(3A)	1.810
Os(2)–H(3A)	1.663	Os(2)–H(4A)	1.398
Os(2)–H(5A)	1.323	Os(1)–H(6A)	1.412
Os(2)–Os(1)–P(1)	119.80(2)	Os(2)–Os(1)–P(2)	130.06(2)
Os(1)–Os(2)–P(3)	126.11(2)	Os(1)–Os(2)–P(4)	119.59(2)
P(1)–Os(1)–P(2)	105.29(3)	P(3)–Os(2)–P(4)	113.76(3)
Os(2)–Os(1)–H(4A)	117.12	Os(2)–Os(1)–H(5A)	120.12
Os(1)–Os(2)–H(6A)	120.38	P(3)–Os(2)–H(4A)	82.97
P(3)–Os(2)–H(5A)	69.22	P(4)–Os(2)–H(4A)	60.04
P(4)–Os(2)–H(5A)	86.13	P(1)–Os(1)–H(6A)	90.92
P(2)–Os(1)–H(6A)	76.20	H(4A)–Os(1)–H(5A)	122.39
Os(1)–H(1A)–Os(2)	95.16	Os(1)–H(2A)–Os(2)	91.91
Os(1)–H(3A)–Os(2)	94.14		

^a Definition of R indices: $R_1 = \sum ||F_o| - |F_c|| / \sum |F_o|$; $wR_2 = [\sum w(F_o^2 - F_c^2)^2 / \sum w(F_o^2)]^{1/2}$.

produced by thermolysis of the appropriate mononuclear hexahydride.³⁹ Compound **2** has also been produced by the reaction of $[\text{OsH}_6(\text{PPh}^i\text{Pr}_2)_2]$ with cyclohexa-1,3-diene in hexane at 328 K.⁴⁰

This deprotonation was initially attempted using piperidine, DBU, and triethylamine, as these bases

(35) Results of a Cambridge Structural Database search for the $\text{Ru}_2(\mu\text{-H})_3$ structural unit.

(36) Abdur-Rashid, K.; Gusev, D. G.; Lough, A. J.; Morris, R. H. *Organometallics* **2000**, *19*, 1652–1660.

(37) Bronger, W.; Sommer, T.; Auffermann, G.; Müller, P. *J. Alloys Compd.* **2002**, *330–332*, 536–542.

(38) Moehring, G. A.; Fanwick, P. E.; Walton, R. A. *Inorg. Chem.* **1987**, *26*, 1861–1866.

(39) Arliguie, T.; Chaudret, B.; Morris, R. H.; Sella, A. *Inorg. Chem.* **1988**, *27*, 598–599.

(40) Steel, C. E.; Spencer, J. L. *unpublished results*.

have been shown to deprotonate rhenium and osmium polyhydrides.^{17,38} However, these attempts were unsuccessful, and deprotonation was only achieved using potassium hydride. This indicates that the pK_a of **1** is greater than that of piperidine- H^+ ,⁴¹ and that **1** is less acidic than the dirhenium polyhydrides $Re_2H_9P_4^+$.³⁸

While isoelectronic ruthenium polyhydrides of the type $Ru_2H_6P_4$ have been shown to possess a non-classical terminal dihydrogen ligand,^{6,39,42} **2** has solely classical terminal hydrides. It is stable under a nitrogen atmosphere rather than displaying the facile exchange of N_2 for H_2 seen in the non-classical ruthenium polyhydrides, and has a nearest contact between terminal hydride ligands of 2.4 Å, significantly longer than even the 1.357(7) Å observed for an elongated non-classical H_2 ligand.⁴³ It has been observed for $Ru_2H_6P_4$ species that replacing PPh_3 with more basic P^iPr_3 ligands induces a change from a non-classical to a classical structure.³⁶ This introduces the possibility that $Os_2H_6P_4$ species with less basic or chelating phosphines may adopt non-classical structures.

Attempts to synthesize the corresponding dinuclear octahydride $Os_2H_8P_4$ from the reaction of **1** with lithium aluminum hydride were unsuccessful.

Significance of Dinuclear Osmium Polyhydrides. As mentioned earlier, the protonation of a mononuclear polyhydride to form a dinuclear polyhydride has previously been observed in rhenium chemistry. Other established transition metal polyhydride chemistry may be transferable to these dinuclear osmium polyhydrides. One such example of this may be the formation of mixed polyhydride-phosphine clusters. Rhenium polyhydrides of the type $Re_2H_8P_4$ have been shown to react with $[Au(PPh_3)]^+$ to form the tri- and tetranuclear clusters $[Re_2H_8(PPh_3)_4Au(PPh_3)]^+$ and $[Re_2H_8(PPh_3)_4\{Au(PPh_3)\}_2]^+$.³⁸ It has been demonstrated that osmium hexahydrides can react with metallic Lewis acids in a similar manner to rhenium heptahydrides,⁹ introducing the possibility that **2** may be able to react with $[Au(PPh_3)]^+$ in the same way as the isoelectronic $Re_2H_8P_4$ to produce a multinuclear polyhydride-phosphine cluster. Hydride-containing transition metal clusters are currently of particular interest, as they often display reversible binding of dihydrogen, giving them relevance in the field of hydrogen storage.⁴⁴

Moreover, osmium polyhydride species such as $[OsH_6(P^iPr_3)_2]$ have been observed to activate sp^2 and sp^3 carbon-hydrogen bonds.^{45,46} Coupled with the observation that multinuclear transition metal polyhydrides can also cleave a variety of C-H and C-C bonds,^{5,47} this gives these new dinuclear osmium polyhydride species potential applications in small molecule activation.

Comparison of Solid State Structures of **1 and **2**.** The structure adopted by **1** in the solid state comprises OsH_2P_2 units

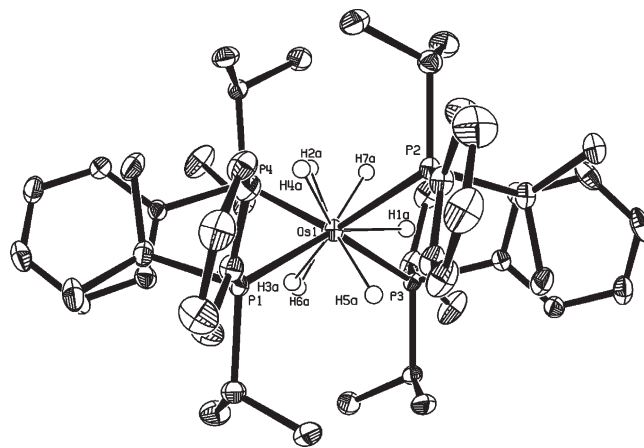


Figure 5. ORTEP diagram of **1** viewed along the Os–Os bond. 50% probability thermal ellipsoids with non-hydride H-atoms and the $HC(SO_2CF_3)_3^-$ anion have been omitted for clarity.

with three bridging hydrides and a non-coordinating anion. The major difference between this structure and similar structures with the $M(\mu-H)_3M$ core is the asymmetry in the molecule. For example, the isoelectronic $[Re_2H_7(PPh_2Me)_4]^-$ contains a center of inversion between the two metal atoms, with the phosphine ligands eclipsed when viewed along the metal–metal bond.⁴⁸ In contrast, the phosphine ligands in **1** are staggered with a torsion angle of 61.8° when viewed along the osmium–osmium bond (Figure 5). This greater degree of asymmetry in **1** compared to similar compounds is most likely due to the steric demand of the PPh^iPr_2 ligands. This leads to **1** having larger P–M–P angles and smaller terminal H–M–H angles when compared to $[Re_2H_7(PPh_2Me)_4]^-$,⁴⁹ as the isopropyl groups force the phosphorus atoms apart, allowing the hydrides to inhabit some of this space. The steric bulk of the ligand introducing torsion about the metal–metal bond is also seen when comparing **2** to its corresponding ruthenium polyhydride $[Ru_2H_6(P^iPr_3)_4]$. Increasing the steric bulk of the ligand from PPh^iPr_2 (cone angle 155°)²⁶ to P^iPr_3 (cone angle 160°)⁵⁰ results in an increase in the torsion angles between phosphine ligands on opposite ends of the molecule (P(2)–Os(1)–Os(2)–P(3) and P(1)–Os(1)–Os(2)–P(4)) from $38.95(4)^\circ$ and $76.49(3)^\circ$ to 57.3° and 79.2° , respectively.³⁶

Compared to the crystal structure of **1**, **2** is less symmetrical about the central $P_2Os-OsP_2$ core because it is composed of $OsHP_2$ and OsH_2P_2 units rather than two OsH_2P_2 units. The OsH_2P_2 unit of **2** is similar to those of **1** with an average Os–P bond length of 2.31 Å (compared to 2.32 Å for **1**) and an average P–Os–P angle of 113.8° (compared to 112.6° for **1**). The $OsHP_2$ unit has a shorter average Os–P bond length (2.27 Å) and a smaller P–Os–P bond angle (105.3°) because of the decreased steric demands of being a seven-coordinate rather than an eight-coordinate center. These differences in the $P_2Os-OsP_2$ core are evident when viewed along the Os–Os bond (Figure 6). In **2**, P(2) is closer to eclipsing P(3) (P–Os–Os–P torsion of $38.95(4)^\circ$) and P(1) is further

(41) Crampton, M. R.; Robotham, I. A. *J. Chem. Res.* **1997**, 22–23.

(42) Precht, M. H. G.; Ben-David, Y.; Giunta, D.; Busch, S.; Taniguchi, Y.; Wisniewski, W.; Görls, H.; Mynott, R. J.; Theyssen, N.; Milstein, D.; Leitner, W. *Chem.—Eur. J.* **2007**, *13*, 1539–1546.

(43) Brammer, L.; Howard, J. A. K.; Johnson, O.; Koetzle, T. F.; Spencer, J. L.; Stringer, A. M. *J. Chem. Soc., Chem. Commun.* **1991**, 241–243.

(44) Weller, A. S.; McIndoe, J. S. *Eur. J. Inorg. Chem.* **2007**, 2007, 4411–4423.

(45) Barrio, P.; Esteruelas, M. A.; Onate, E. *Organometallics* **2004**, *23*, 3627–3639.

(46) Baya, M.; Eguillor, B.; Esteruelas, M. A.; Lledos, A.; Olivan, M.; Onate, E. *Organometallics* **2007**, *26*, 5140–5152.

(47) Shima, T.; Ichikawa, T.; Suzuki, H. *Organometallics* **2007**, *26*, 6329–6337.

(48) Hinman, J. G.; Abdur-Rashid, K.; Lough, A. J.; Morris, R. H. *Inorg. Chem.* **2001**, *40*, 2480–2481.

(49) For **1**, avg P–Os–P = 112.64° , avg H–Os–H = 119.04° . For $[Re_2H_7(PPh_2Me)_4]^-$, P–Re–P = 105.70° , H–Re–H = 136.86° .

(50) Tolman, C. A. *Chem. Rev.* **1977**, *77*, 313–348.

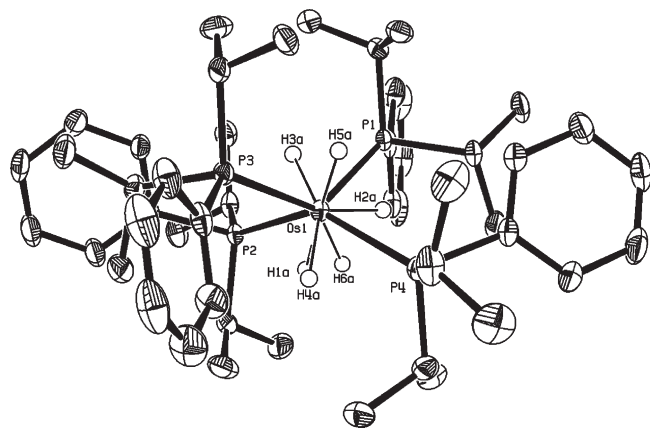


Figure 6. ORTEP diagram of **2** viewed along the Os–Os bond. 50% probability thermal ellipsoids with non-hydride H-atoms omitted for clarity.

staggered from P(4) (P–Os–Os–P torsion of $76.49(3)^\circ$), creating a compound with two distinct P–Os–Os–P faces.

However, it is **1** that is asymmetric about the ends of the molecule. In **1**, Os(1) has PPh^iPr_2 ligands which are oriented with the isopropyl groups pointing inward (toward the $\text{Os}_2(\mu\text{-H})_3$ core), while Os(2) has PPh^iPr_2 ligands in which the phenyl groups point inward, appearing to be π -stacked (closest C–C contact of 3.2 Å between C(2) and C(14)). This means the P–Os–P angle for Os(2) is very slightly larger than for Os(1), $113.00(2)^\circ$ compared to $112.28(2)^\circ$. This difference between the two ends of the molecule may be a consequence of having to accommodate the $\text{HC}(\text{SO}_2\text{CF}_3)_2^-$ counterion into the crystal packing. In the neutral **2**, both ends of the molecule have one phosphine with a phenyl group pointing inward and one with an isopropyl group pointing inward, providing a

degree of symmetry between the two ends of the molecule, and giving the OsP_2H_2 unit of **2** a larger P–Os–P angle of $113.76(3)^\circ$.

Conclusion

In this paper we report the synthesis of two dinuclear osmium polyhydrides with a high hydride count. We have synthesized the dinuclear polyhydride $[\text{Os}_2\text{H}_7(\text{PPh}^i\text{Pr}_2)_4][\text{HC}(\text{SO}_2\text{CF}_3)_2]$ (**1**) from the protonation of $[\text{OsH}_6(\text{PPh}^i\text{Pr}_2)_2]$ with $\text{H}_2\text{C}(\text{SO}_2\text{CF}_3)_2$. This is a rare example of the protonation of an osmium polyhydride resulting in a dinuclear structure, with this reactivity being attributed to facile loss of H_2 from the observed intermediate $[\text{OsH}_3(\text{H}_2)_2(\text{PPh}^i\text{Pr}_2)_2]^+$ (**3**). The cationic species **1** can also be deprotonated with potassium hydride to yield the first dinuclear hexahydride $[\text{Os}_2\text{H}_6(\text{PPh}^i\text{Pr}_2)_2]$ (**2**). X-ray diffraction study reveals both **1** and **2** to be classical polyhydrides with a $\text{P}_2\text{Os}(\mu\text{-H})_3\text{OsP}_2$ core and a staggered arrangement of the phosphine ligands.

These species represent the extension of established rhenium and ruthenium chemistry to high hydride count osmium polyhydrides. This may provide the potential to adapt successful polyhydride chemistry to similar osmium species, which have demonstrated utility in reactions such as C–H activation.

Acknowledgment. We thank Dr Jan Wikaira at the University of Canterbury for collecting the single crystal X-ray data.

Supporting Information Available: X-ray crystallographic files in CIF format for $[\text{Os}_2\text{H}_7(\text{PPh}^i\text{Pr}_2)_4][\text{HC}(\text{SO}_2\text{CF}_3)_2]$ (**1**) and $[\text{Os}_2\text{H}_6(\text{PPh}^i\text{Pr}_2)_2]$ (**2**). This material is available free of charge via the Internet at <http://pubs.acs.org>.